Inferring individual rules from collective behavior

Ryan Lukeman[a,1], Yue-Xian Li[b], and Leah Edelstein-Keshet[b]

[a]Department of Mathematics, Statistics, and Computer Science, St. Francis Xavier University, Antigonish, NS, Canada B2G 2W5; and [b]Department of Mathematics, University of British Columbia, Vancouver, BC, Canada V6T 1Z2

Edited* by Simon A. Levin, Princeton University, Princeton, NJ, and approved May 27, 2010 (received for review February 17, 2010)

Social organisms form striking aggregation patterns, displaying cohesion, polarization, and collective intelligence. Determining how they do so in nature is challenging; a plethora of simulation studies displaying life-like swarm behavior lack rigorous comparison with actual data because collecting field data of sufficient quality has been a bottleneck. Here, we bridge this gap by gathering and analyzing a high-quality dataset of flocking surf scoters, forming well-spaced groups of hundreds of individuals on the water surface. By reconstructing each individual's position, velocity, and trajectory, we generate spatial and angular neighbor-distribution plots, revealing distinct concentric structure in positioning, a preference for neighbors directly in front, and strong alignment with neighbors on each side. We fit data to zonal interaction models and characterize which individual interaction forces suffice to explain observed spatial patterns. Results point to strong short-range repulsion, intermediate-range alignment, and longer-range attraction (with circular zones), as well as a weak but significant frontal-sector interaction with one neighbor. A best-fit model with such interactions accounts well for observed group structure, whereas absence or alteration in any one of these rules fails to do so. We find that important features of observed flocking surf scoters can be accounted for by zonal models with specific, well-defined rules of interaction.

flocking | individual tracking | model/data | surf scoters | animal groups

Many social organisms exhibit cohesive, self-organized group motion with visually compelling aggregation patterns (1). Investigating how behavior at one scale (the individual) engenders behavior on the higher scale (e.g., the swarm) has spawned a rich field of research, driven largely by simulation and modeling of both physical (2–4) and biological (5–9) systems. One consensus is that even simple individual rules can give rise to complex group behavior. However, whether/which groups have leaders, how neighbors are surveyed by each member, what is the relative effect of local versus global information, and whether interactions affect speed, turning angles, acceleration, or all of the above is unclear for most flocks. What underlying rules of behavior are at play in real swarms or flocks remains a long-standing question that motivates our study.

Given the rich diversity of theoretical models that assume distinct forces and reactions, it is of great interest to assess which correspond to actual behavior in nature. Yet simulation studies alone cannot tackle this question because patterns similar to observations can be generated by different model mechanisms. Instead, this question requires a close comparison between real and model social aggregates and measurement of what individuals are actually doing within large groups, as is our focus here.

Technological difficulties in tracking individuals accurately in fast-moving groups presents a challenge (10). Recovering the spatial structure of large groups is hampered by obstruction of the view into the group interior (occlusion) in three dimensions, a problem that is compounded by large group sizes. Yet, without complete reconstruction of positions, individual trajectories cannot be teased out from successive images of the group. Because of these limitations, previous empirical work on birds (11–13), insects (14), and fish (15) has been restricted to small groups, and resulted in smaller, noisier datasets.

Advances in digital imaging have led to refinement in both the spatial and temporal dimension of the data. Automated tracking of (up to 120) locusts in a 2D laboratory setting has revealed density-dependent transitions from disordered groups to highly aligned groups (16), and cannibalistic interactions driving collective motion (17). Recent work (18) on huge starling flocks (>1,000 birds) increased by an order of magnitude the size of groups considered over previous studies. There, average local swarm velocities (rather than individual tracks) could be quantified because of occlusion, speed, and numerosity of the birds. Other recent work (19, 20) using automated tracking software for schooling fish has led to accurate long-time trajectory reconstruction for individuals in small groups (four to eight fish). Long-distance trajectories have also been constructed for a flock of up to 10 homing pigeons by using GPS tracking (10). Here, we report on a dataset and modeling of flocks of hundreds of surf scoters (*Melanitta perspicillata*).

Given a good dataset, it is not always clear a priori which model framework is suitable for testing hypothetical mechanisms of interaction against the data. Two main approaches exist: (*i*) topological-distance models, in which each (interior) individual interacts with a fixed number of neighbors, versus (*ii*) metric-distance models, in which the individual interacts with all neighbors within a certain distance. Many metric-distance models are "zonal"; that is, interaction forces are implemented through a series of layered zones (repulsion, alignment, attraction, respectively) around a given individual. The zone in which a neighbor is found determines which of these interactions takes place, and the shape and structure of zones reflect sensory characteristics of each individual. Zonal models have revealed much about collective motion: dynamic switching between collective patterns (8), effects of leadership on uninformed members (9), and how group size (21, 22), number of neighbors (6, 21), and heterogeneity in members (23) influence emergent group properties such as shape, density, and polarization of the group. Apart from evidence for topological interactions in airborne starling flocks (18), and empirical evidence for attraction/repulsion zones in fish schools (24), the validity of zonal models for different animal groups has not been carefully assessed thus far.

We report here combined efforts of collecting and analyzing data for large flocks of scoters, and modeling the most important features of such flocks derived from the data. As shown here, this work has enabled us to pinpoint specific rules underlying observed features. The results suggest that zonal models based on metric distance are an appropriate tool for generating insight into the mechanisms of collective motion.

Results

Surf scoters overwinter in shallow coastal areas of North America in flocks numbering hundreds of individuals. Flocks collectively moving on the water surface before diving to forage on mollusks (25) exhibit a high degree of cohesion, polarization, well-defined

Author contributions: R.L., Y.-X.L., and L.E.-K. designed research; R.L. performed research; R.L. analyzed data; and R.L. and L.E.-K. wrote the paper.

The authors declare no conflict of interest.

*This Direct Submission article had a prearranged editor.

[1]To whom correspondence should be addressed. E-mail: rlukeman@stfx.ca.

This article contains supporting information online at www.pnas.org/lookup/suppl/doi:10.1073/pnas.1001763107/-/DCSupplemental.

spacing structure, and synchrony in dives (26, 27) (Fig. 1*A* and *SI Text*).

In our data, individuals have a mean nearest-neighbor distance (NND) of 1.45 body lengths (BL) with SD 0.25 BL, and a mean speed of 2.0 BL/s. While collecting data, we noted that ducks occasionally accelerate/decelerate and are visually alert to their neighbors (in 360°), displaying frequent head turns. Kleptoparasitic gulls (28) (primarily glaucous-winged gulls, *Larus glaucescens*) frequently attack scoters, robbing them of mussels (*Mytilus edulis*) (26). We observed scoters actively avoiding encroaching gulls by forming avoidance zones ("vacuoles") within the aggregate (Fig. S1).

Noteworthy features of the dataset we collected are a natural setting using native undomesticated birds, and minimal effect of measurement on behavior, large groups (up to ≈200), and convenient geometry (2D, well-spaced floating flock, versus 3D flying swarm). The high signal-to-noise ratio allows us to reconstruct individual trajectories accurately.

The observed mean neighbor density and angular deviation obtained by pooling the data are depicted in the 2D plot (Fig. 2 *A* and *B*). The neighbor density (Fig. 2*A*) reveals an empty disk (dark blue), surrounded by ring of high density (red) at 1.45 BL, and further clouds of lower density (yellow). The highest density (dark red) occurs at a preferred distance directly in front/behind the focal bird (Fig. 4*C*). A few "echo" waves are seen in radial neighbor density plots (Fig. 4*D*). These observations imply a higher probability of finding a neighbor at preferred distance and angle.

The mean angle between headings (denoted "absolute deviation") is shown in Fig. 2*B*. At close distances (< ≈1.3 BL), deviation is strongly angle-dependent (high in front/behind: dark red; low at left/right: blue): That is, birds align roughly in parallel with neighbors alongside, but deviate from neighbors in the axis of motion. At preferred distances (≈1.5 BL), deviation is low at all angles (minimal at left/right). At larger distances (>2 BL), deviation increases as correlation decays.

As shown in Fig. 2, neighbor distributions have circular reflective symmetry due to mutual neighbor pairs. We asked whether the front/back high deviation stems from interactions from behind

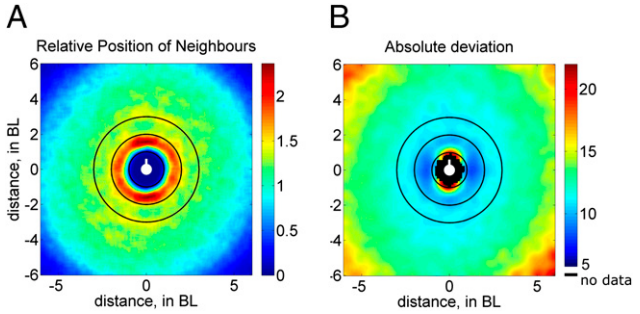

Fig. 2. Results of data analysis: Density maps for position and orientation of neighbors relative to a typical individual (central white disk, with "beak" in front) based on pooled data excluding flock edges. Radial distances of 1, 2, and 3 BL are superimposed. (*A*) Density of neighbor positions (normalized to have an average value of 1) showing a preference for frontal neighbors. (*B*) Relative neighbor orientation showing high deviation in front/behind versus low at left/right flanks. Deviation increases radially outwards, indicating local alignment interaction (as distinct from alignment to common goal).

(avoiding aggressive neighbors), from the front (collision avoidance), or both. The deviation from the mean velocity field caused by a neighbor too close in front was higher than that of a neighbor too close in back, suggesting that a frontal response dominates (further discussion in *SI Text*).

Taken together, Fig. 2 *A* and *B* suggest that the dominant distance-dependent interaction occurs along the axis of motion: Individuals preferentially move in line with those in front of them, and repel strongly, by deviating sideways, if too close to that neighbor. In contrast, alignment with neighbors is strongest for neighbors at left/right. Importantly, the increase in deviation with radial distance in Fig. 2*B* gives direct evidence for the existence of a local alignment force, for if alignment was instead imparted solely by global information (e.g., the direction to the foraging site), deviation would be uncorrelated with distance from a given individual.

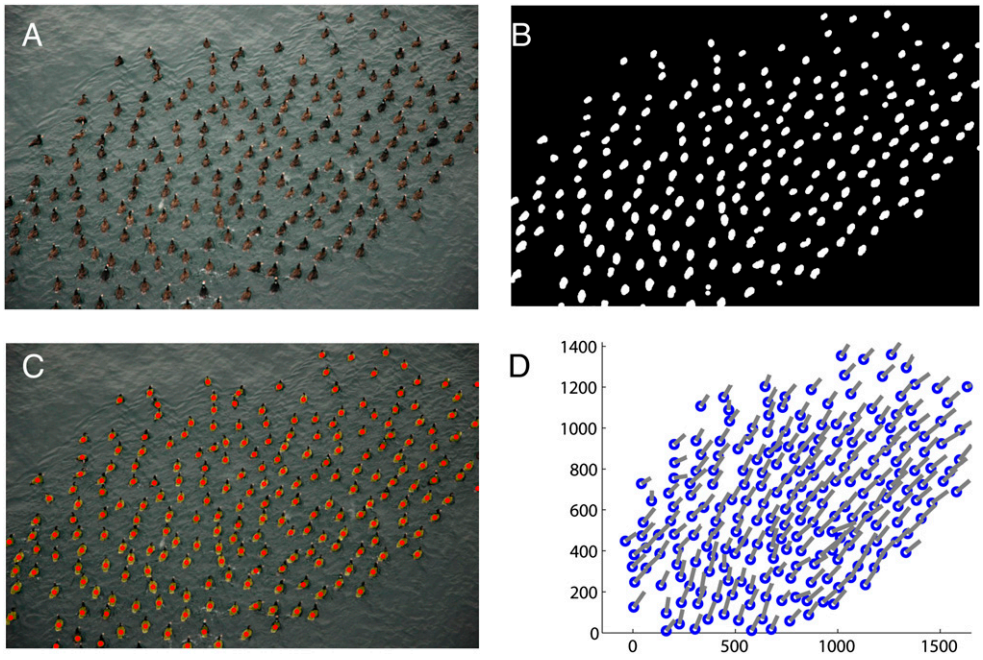

Fig. 1. A typical flock of *M. perspicillata* (surf scoter) moving on the water surface showing a raw image (*A*) and an image filtered and thresholded to isolate individuals and eliminate noise (*B*). (*C*) Validation of objects by overlay on original image; centers of mass for individuals were calculated. (*D*) Correction for perspective and transformation to "real" positions, calculated velocities (gray lines), and correction for drift currents.

Results of aggregate data analysis were fitted to a hierarchy of individual-based zonal models (5–9, 22) with space around an individual partitioned into zones of repulsion, alignment, and attraction. The clearly observed concentric zones in the data motivated this choice of model framework, and observed zone radii were used as input parameters in the zonal models. For x = distance to neighbor, we assumed piecewise linear pairwise-interaction forces with magnitude $g(x)$ normalized ($-1 \le g(x) \le 1$), and weighted by tunable parameters, ω_k (k = attraction, repulsion, etc.). For n individuals with position $\vec{x}_i$ and velocity $\vec{v}_i$ ($i = 1, \ldots, n$), our Lagrangian model (4, 29) is

$$\frac{d\vec{x}_i}{dt} = \vec{v}_i,$$
$$\frac{d\vec{v}_i}{dt} = \vec{f}_{i,aut} + \vec{f}_{i,\mathrm{int}} + \vec{\xi}_i$$

with $\vec{f}_{i,int}$ the attraction/alignment/repulsion force, $\vec{f}_{i,aut}$ an autonomous self propulsion, and $\vec{\xi}_i$ (Gaussian) noise. Environmental cues are included by setting $\vec{f}_{i,aut} = \vec{a} - \gamma\vec{v}_i$, with $\vec{a}$ an intrinsic velocity toward a foraging goal and $\gamma\vec{v}_i$ a drag as in ref. 4. The choice of this nonconstant velocity model version stems from our field observations that individual ducks accelerate from time to time. The motion of each model duck is based on the sum of forces averaged over neighbors in each zone, except for frontal interaction, described below.

Behavior of the model depends strongly on the assumptions about the sum of interaction forces, $\vec{f}_{i,int}$. We tested a sequence of models from simple attraction/repulsion (A/R) in concentric rings to more detailed variants, with/without blind angles, and with a hierarchy of decisions within the zones (8, 9).

Simple A/R alone (7, 30–32) (Fig. 3*A*) captures the radial distribution of neighbors but fails to account for angular preference for neighbors in front. Including alignment forces (attraction/repulsion/alignment, A/R/A model; Fig. 3*B*) (4, 6, 8, 22) improves the match but fails to account for the observed bias in the angular distribution over a wide range of parameters we tested (using optimization similar to the procedure described below and in *SI Text*).

We asked what influences could account for the observed frontal bias of neighbors. Inclusion of a rear blind sector (6, 8) in the A/R/A model was rejected, because it led to increased density of neighbors at left/right (Fig. 3*C*), in contrast to the front/back bias observed in the data. (Observed frequent head-turning of individual birds also suggests that blind angles are unlikely.) Weighting A/R magnitude toward the front in A/R/A creates frontal preference with an unrealistic elliptical repulsion zone (Fig. 3*D*) contrary to the observed pattern in Fig. 2*A* and, hence, was rejected. Alternatively, modifying the structure of attraction zones in A/R/A from circular to elliptical (elongated to the front by up to a factor of 2) had no effect on resulting neighbor distributions (i.e., Fig. 3*B*).

Rather, including an A/R frontal interaction with (up to) one nearest neighbor in a sector of $\theta \pm 30°$ (Fig. 4*A*) shows a good fit (Fig. 3*E*) to observed neighbor distribution and angular preference. The qualitative agreement is robust to parameter variations, as discussed further on. Fig. 4*A* summarizes the best candidate model, suggesting that individuals within flocks balance A/R/A interactions in all directions, but also attract/repel from the single nearest neighbor directly ahead.

To determine the relative contributions of interactions (attraction, repulsion, alignment, frontal interaction) and noise to observed behavior, we write each in terms of a "normalized" force, weighted by relative strengths,

$$\vec{f}_{i,int} = \omega_{rep}\vec{f}_{i,rep} + \omega_{att}\vec{f}_{i,att} + \omega_{al}\vec{f}_{i,al} + \omega_{front}\vec{f}_{i,front},$$

where ω_{rep}, ω_{att}, ω_{al}, and ω_{front} are weighting parameters to be fitted. (See *SI Text* for details.)

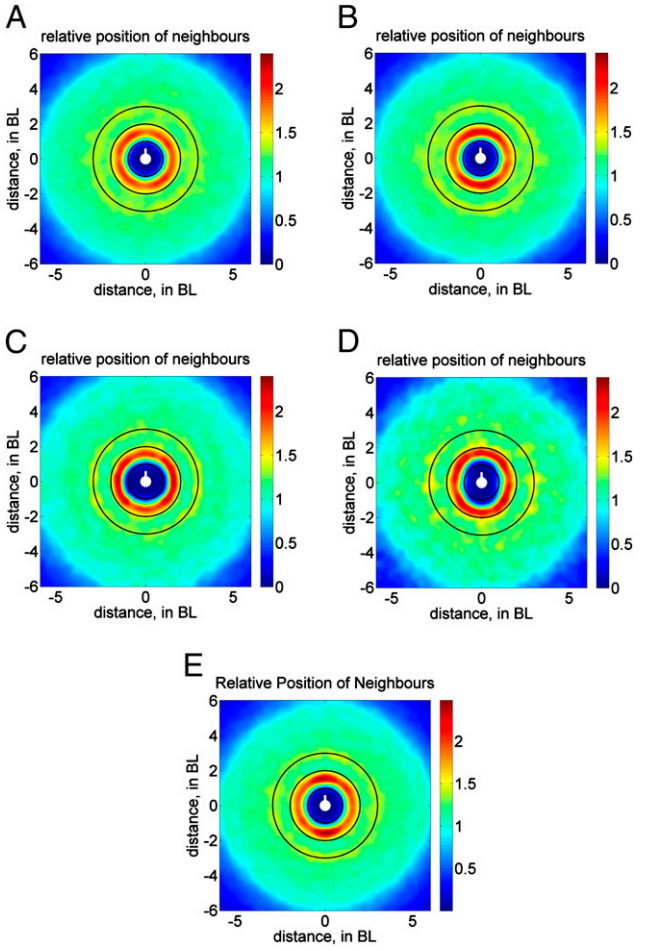

Fig. 3. Results of model predictions: Neighbor distribution plots (as in Fig. 2*A*) for a sequence of models (details in *SI Text*). Simple attraction-repulsion (A/R) (*A*), with alignment (A/R/A) (*B*), A/R/A with 45° blind angle in back (*C*), A/R/A with angle-dependent weighting $\exp(w\cos(\theta_{ij}))/\exp(w)$, where θ_{ij} is the relative angle between neighbors, and $w = 2$ is a weighting parameter (*D*), A/R/A model with additional frontal interaction, ($\theta \pm 30$) (*E*). Each distribution was calculated from 20 model simulations of 100 individuals, with random initial conditions. Radial distances of 1, 2, and 3 BL are superimposed.

We carried out parameter optimization to match model predictions to data. Our goodness-of-fit measure is the sum of two errors: the mean-squared difference of observed and predicted (*i*) 2D neighbor densities (Fig. 2*A* and 3*E*, respectively) and (*ii*) density as a function of circumferential position in an annulus at the preferred distance (Fig. 4*C*). Ranges for ω values were first established by numerical exploration, then optimized by a random-search algorithm with the above objective criterion. Optimal parameters (Fig. 4*B*) produce the distribution of Fig. 3*E* and radial plots (solid curves in Fig. 4 *C* and *D*) that match the corresponding observations (Fig. 2*A*, and dotted curves in Fig. 4 *C* and *D*). Optimality was verified by varying each parameter about its optimum (Fig. 4*B Inset*).

Optimization reveals that short-range repulsion is an order of magnitude greater than net attraction in the attraction zone. Interestingly, although ω_{front} is two orders of magnitude lower than repulsion, and clearly a relatively weak effect, it has a noticeable effect on neighbor angular preference. The optimal alignment parameter ω_{al} is the same order as the magnitude of self-propulsion ($|\vec{a}| = 0.5$ in simulations). Our results suggest that individuals balance the tendency to "follow-the-leader" and align with neigh-

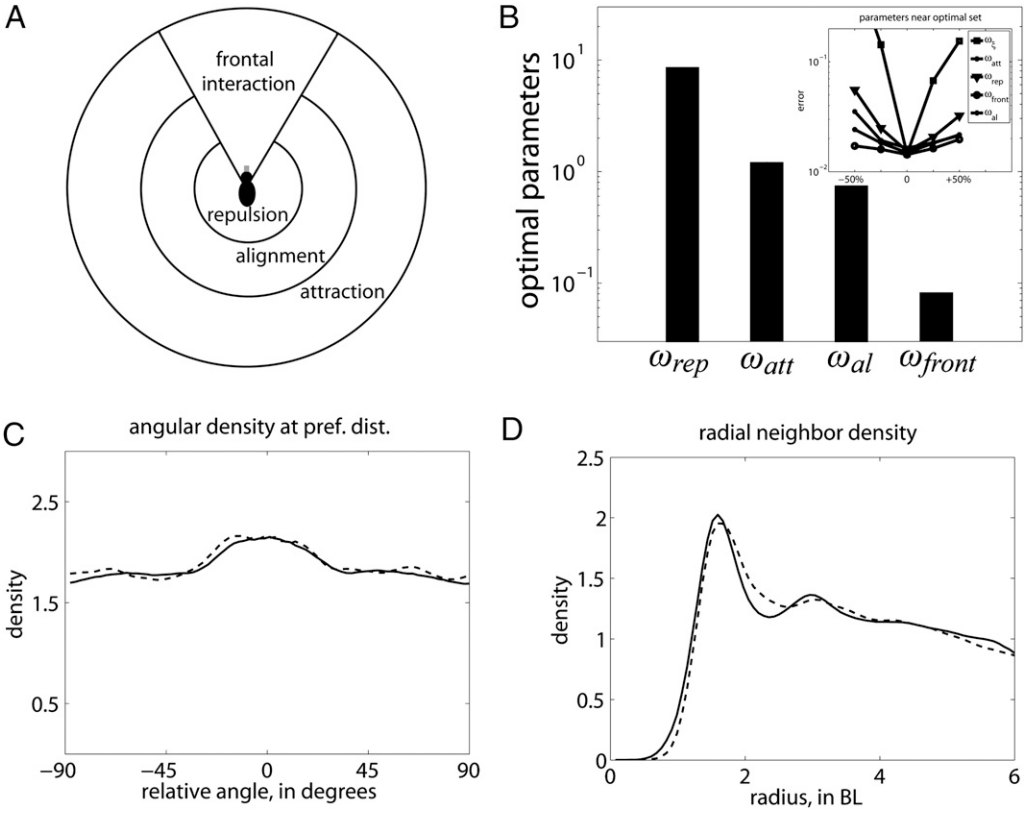

Fig. 4. Individual behavior inferred by matching model to data. Individuals obey a hierarchy of repulsion, alignment, and attraction to neighbors in zones shown in *A*, supplemented by A/R with one neighbor in a frontal interaction sector. (*B*) Relative magnitudes of repulsion, attraction, alignment, and frontal forces (ω_k) obtained by optimizing the model fit to data (logarithmic scale). (*B Inset*) Evidence for optimality shown by varying each parameter about its best-fit value. Ranges explored were −50% to +50% of the optimal parameter set (ω_{rep} = 8.5, ω_{att} = 1.2, ω_{al} = 0.74, ω_{front} = 0.08, and ω_{ξ} = 0.37). (*C*) Density of neighbors vs. angle $-90° \leq \theta \leq 90°$ at 1.5 BL (the preferred distance) showing good agreement between model (solid) and data (dotted) (0° is to the front). (*D*) A comparison of radial neighbor density for data (dotted) and model (solid).

bors with their response to external cues (direction to foraging site) and strong spacing behavior.

Discussion

In this paper we collected, digitized, and analyzed a large dataset for flocks of surf scoters and used it to reverse-engineer underlying individual rules. Our work bridges the gap between previous studies by accurately reconstructing individual tracks (and hence velocities, neighbor distances, etc.) in groups numbering hundred(s) of members.

Our dataset allowed for deeper probing of individual rules underlying group behavior. Accurate reconstruction of individual positions, trajectories, and velocities reveal a distinct 2D structure ("heat map") in relative spatial distribution of neighbors. This structure indicates a preference for neighbors directly behind and in front (at ≈1.5 BL away), alignment with neighbors on each side, and active avoidance of those in front (by sideways diversion). Such conclusions would be difficult to quantify without the individual tracking reported herein.

Comparing such observations against predictions of a sequence of Lagrangian models, we rejected null hypotheses (simple A/R, blind angles, frontal weighting of interactions) that disagreed qualitatively with the dataset. An A/R/A model complemented by weak frontal interactions predicts behavior that is consistent with observations. As shown in ref. 31, general properties of A/R forces (e.g., monotonicity, relative magnitudes, etc.) matter more than specific details in determining cohesiveness and spacing in groups. Using piecewise linear forces with discrete zones simplified the parametrization of the model because zone radii were directly observable in the data.

Optimization of parameters (relative weights of forces) reveals that repulsion dominates over other forces, with attraction and alignment tendencies roughly of equal (and lower) magnitudes. Overall, our work illustrates that zonal models can lead to insight about how individual rules lead to observed flock behavior.

Most empirical studies of animal groups report structure in both nearest-neighbor spacing and relative bearings. In fish schools, individuals are observed to preferentially occupy either lateral (19, 33) or diagonal positions (11, 34) relative to neighbors, avoiding positions directly in front or behind. Similarly, observations of airborne bird flocks (12, 18) reveal avoidance of nearest neighbors directly in the path of an individual's motion. A number of mechanisms have been put forth to explain this angular structure (35), including hydro/aerodynamic benefits, anisotropic vision, or avoidance of collisions caused by changing speeds.

Our findings for 2D flocks contrast with the above, in that we observe, on average, a peak of density directly in front/behind each individual. Given this departure from previous observations, one might ask why such a difference arises. One explanation is that surface-swimming surf scoters move much more slowly than schooling fish or airborne birds. This fact implies a reduced risk of collision with those just ahead, and so a reduction in the penalty for being too close to a neighbor in the path of motion. A second factor is that our flocks move in 2D on the water surface, so that aero/hydrodynamic effects are bound to be distinct from those encountered by flying birds and swimming fish. Thus, aerodynamic benefits associated with bird flight should not be ex-

trapolated to such flocks. Because the impact due to collisions is less significant, and the threat of predation or parasitism by gulls more imminent, placing a neighbor directly ahead may be a more beneficial "selfish herd" strategy in areas near the foraging sites that tend to be frequented by gulls. Finally, the occlusion of the visual field caused by a frontal neighbor is compensated by frequent head-turning, a behavior that could be less suitable in rapid flight.

Although the ecological implications of such behavior remains to be more fully explored, we conjecture that the tendency to follow the leader could facilitate targeted foraging on localized patches of sessile prey (27). Further, attraction to flockmates likely affords protection (e.g., from kleptoparasitic gulls; ref. 26), while maximizing reliance on informed members at the edge of the group (9). The observed spacing patterns of scoters could facilitate orderly "queuing" that promotes more efficient foraging or could be related to other elements of locomotion or flock dynamics. Alignment, spacing, and sequential/synchronous dives could potentially decrease the chance of underwater interference with flockmates, influence diving energetics, or facilitate extracting prey from the substrate. Coordination of underwater diving activities among individuals remains an important area for empirical research.

Evidence from casual observations suggests that flocking parameters (magnitudes of forces and sizes of zones) are adaptable, adjusting dynamically to the environment and changing state of the flock. We observe wider interspecies repulsion zones (e.g., when gulls infiltrate the flock). Alignment is lost and spacing changes between foraging bouts. In gathering this data, we observed occasional flock transitions (polarized, nonpolarized, etc.), implying that group parameters likely vary dynamically over a range of values depending on circumstances (see also ref. 8).

The data analysis tools we have developed here can be used to study other swimming flocks (e.g., eider ducks, Barrow's goldeneyes). The comparative analysis of species-specific differences would address questions on the universality (or specificity) of individual rules, how they vary with conditions, within and between groups. The continued close marriage of theoretical modeling and empirical data will be indispensable as such questions are tackled.

Materials and Methods

Time series of 2D flocks at Burrard Inlet, Vancouver, BC, were recorded by oblique overhead photography. A fixed landmark (the edge of a dock) defined coordinates for distance calibration. Data were gathered over a 2-wk period in March 2008, and 13 separate sequences of group motion were reconstructed. Each sequence was comprised of 25–137 frames at 3 frames per second, with up to 200 individuals per frame. In total, >75,000 positions were reconstructed. Frames were digitized (Fig. 1 *A*–*C*), and positions in successive frames were matched by using customized particle-tracking software, giving a timecourse of individual positions, velocities, and headings (Fig. 1*D*). Images were corrected for perspective distortion and velocities were adjusted for water currents by using intrinsic fluid markers. Edge individuals were excluded from the analysis. Relative positions (Fig. 2*A*) and heading deviations (Fig. 2*B*) were computed. (See *SI Text* for a detailed description of methods. Also, see Figs. S2–S8, Table S1, Movie S1, Movie S2, and Movie S3 for additional details.)

ACKNOWLEDGMENTS. We thank D. Grunbaum, R. Ydenberg, and J. Heath for discussions. Computational facilities are provided by ACEnet, the regional high-performance computing consortium for universities in Atlantic Canada. This work was funded by Natural Sciences and Engineering Council of Canada (NSERC) discovery grants (to L.E.-K. and Y.-X.L.) and an accelerator NSERC grant (to L.E.-K.). R.L. was funded by an NSERC postgraduate fellowship, a University of British Columbia graduate fellowship, and an International Graduate Training Center fellowship provided by the Pacific Institute for the Mathematical Sciences. L.E.-K. has been a Distinguished Scholar in residence at the Peter Wall Institute for Advanced Studies.

1. Parrish JK, Edelstein-Keshet L (1999) Complexity, pattern, and evolutionary trade-offs in animal aggregation. *Science* 284:99–101.
2. Vicsek T, Czirók A, Ben-Jacob E, Cohen I, I, Shochet O (1995) Novel type of phase transition in a system of self-driven particles. *Phys Rev Lett* 75:1226–1229.
3. Czirók A, Vicsek M, Vicsek T (1999) Collective motion of organisms in three dimensions. *Physica A* 264:299–304.
4. Levine H, Rappel WJ, Cohen I (2001) Self-organization in systems of self-propelled particles. *Phys Rev E Stat Nonlin Soft Matter Phys* 63:017101.
5. Sakai S (1973) A model for group structure and its behavior. *Biophysics* 13:82–90.
6. Huth A, Wissel C (1992) The simulation of movement of fish schools. *J Theor Biol* 156: 365–385.
7. Gueron S, Levin SA, Rubenstein DI (1996) The dynamics of herds: From individuals to aggregations. *J Theor Biol* 182:85–98.
8. Couzin ID, Krause J, James R, Ruxton GD, Franks NR (2002) Collective memory and spatial sorting in animal groups. *J Theor Biol* 218:1–11.
9. Couzin ID, Krause J, Franks NR, Levin SA (2005) Effective leadership and decision-making in animal groups on the move. *Nature* 433:513–516.
10. Nagy M, Ákos Z, Biro D, Vicsek T (2010) Hierarchical group dynamics in pigeon flocks. *Nature* 464:890–893.
11. Cullen J, Shaw E, Baldwin H (1965) Methods for measuring the three-dimensional structure of fish schools. *Anim Behav* 13:534–543.
12. Major PF, Dill LM (1978) The three-dimensional structure of airborne bird flocks. *Behav Ecol Sociobiol* 4:111–122.
13. Pomeroy H, Heppner F (1992) Structure of turning in airborne rock dove (Columba livia) flocks. *Auk* 109:256–267.
14. Okubo A, Chiang H (1974) An analysis of the kinematics of swarming of Anarete pritchardi Kim (Diptera: Cecidomyiidae). *Res Popul Ecol (Kyoto)* 16:1–42.
15. Pitcher TJ, Partridge BL (1979) Fish school density and volume. *Mar Biol* 54:383–394.
16. Buhl J, et al. (2006) From disorder to order in marching locusts. *Science* 312:1402–1406.
17. Bazazi S, et al. (2008) Collective motion and cannibalism in locust migratory bands. *Curr Biol* 18:735–739.
18. Ballerini M, et al. (2008) Interaction ruling animal collective behavior depends on topological rather than metric distance: Evidence from a field study. *Proc Nat Acad Sci USA* 105:1232–1237.
19. Grunbaum D, Viscido S, Parrish J (2004) Extracting interactive control algorithms from group dynamics of schooling fish. *Coop Control LNCIS* 309:103–117.
20. Viscido SV, Parrish JK, Grunbaum D (2004) Individual behaviour and emergent properties of fish schools: A comparison of observation and theory. *Mar Ecol Prog Ser* 273: 239–249.
21. Viscido SV, Parrish JK, Grunbaum D (2004) The effect of population size and number of influential neighbors on the emergent properties of fish schools. *Ecol Modell* 183: 347–363.
22. Kunz H, Hemelrijk CK (2003) Artificial fish schools: Collective effects of school size, body size, and body form. *Artif Life* 9:237–253.
23. Hemelrijk CK, Kunz H (2004) Density distribution and size sorting in fish schools: An individual-based model. *Behav Ecol* 16:178–187.
24. Tien J, Levin S, Rubenstein D (2004) Dynamics of fish shoals: Identifying key decision rules. *Evol Ecol Res* 6:555–565.
25. Savard J-P, Bordage D, Reed A (1998) Surf Scoter (Melanitta perspicillata). *The Birds of North America No. 363*, eds Poole A, Gill F (Birds of N Am, Philadelphia).
26. Schenkeveld LE, Ydenberg RC (1985) Synchronous diving by surf scoter flocks. *Can J Zool* 63:2516–2519.
27. Beauchamp G (1992) Diving behavior in surf scoters and Barrow's goldeneyes. *Auk* 109:819–827.
28. Brockmann HJ, Barnard CJ (1979) Kleptoparasitism in birds. *Anim Behav* 27:487–514.
29. Okubo A (1980) *Diffusion and Ecological Problems: Mathematical Models* (Springer, New York).
30. Warburton K, Lazarus J (1991) Tendency-distance models of social cohesion in animal groups. *J Theor Biol* 150:473–488.
31. Mogilner A, Edelstein-Keshet L, Bent L, Spiros A (2003) Mutual interactions, potentials, and individual distance in a social aggregation. *J Math Biol* 47:353–389.
32. D' Orsogna MR, Chuang YL, Bertozzi AL, Chayes LS (2006) Self-propelled particles with soft-core interactions: patterns, stability, and collapse. *Phys Rev Lett* 96:104302.
33. Partridge BL (1982) The structure and function of fish schools. *Sci Am* 246:114–123.
34. Partridge BL, Pitcher T, Cullen JM, Wilson J (1980) The three-dimensional structure of fish schools. *Behav Ecol Sociobiol* 6:277–288.
35. Ballerini M, et al. (2008) An empirical study of large, naturally occurring starling flocks: A benchmark in collective animal behaviour. *Anim Behav* 76:201–215.